Journal of Luminescence 198 (2018) 24–27

Contents lists available at ScienceDirect

Journal of Luminescence

journal homepage: www.elsevier.com/locate/jlumin

Observation of a Te^{4+} center with broad red emission band and high fluorescence quantum efficiency in TeO_2-Li_2O glass

F.B. Costa[a], A.K.R. Souza[a], A.P. Langaro[a], J.R. Silva[a], F.A. Santos[b], M.S. Figueiredo[b], K. Yukimitu[c], J.C.S. Moraes[c], L.A.O. Nunes[d], L.H.C. Andrade[a], S.M. Lima[a,*]

[a] Grupo de Espectroscopia Óptica e Fototérmica, Universidade Estadual de Mato Grosso do Sul, C. P. 351, 79804-970 Dourados, MS, Brazil
[b] Grupo de Pesquisa de Materiais Fotônicos e Energia Renovável, Universidade Federal da Grande Dourados, 79804-970 Dourados, MS, Brazil
[c] Grupo Vidros e Cerâmicas, Faculdade de Engenharia de Ilha Solteira – UNESP, Ilha Solteira, SP, Brazil
[d] Laboratório de Laser e Aplicações, Universidade de São Paulo, C. P. 369, 13560-970 São Carlos, SP, Brazil

ARTICLE INFO

Keywords:
Te^{4+} center
Lithium tellurite glass
Fluorescence quantum efficiency
Thermal lens spectrometry

ABSTRACT

In this work, a lithium tellurite glass ($80TeO_2 - 20Li_2O$, in mol%) was synthesized and its optical properties were analyzed. This glass matrix has been extensively studied, mainly due to its highly nonlinear optical properties, but there have been no reports concerning its luminescence properties. To the best of our knowledge, this is the first observation of visible emission related to Te^{4+} centers in a lithium tellurite glass. A broad and intense emission band was centered at 650 nm and there was a broad excitation band in the UV–Vis region. The emission lifetime at room temperature was approximately 7.0 ± 0.2 μs and the fluorescence quantum efficiency was 63 ± 6%. These characteristics indicated that the system consisting of Te^{4+} centers in lithium tellurite glass is a good candidate as a phosphor material for various applications.

1. Introduction

Tellurite (TeO_2-based) glasses are of scientific and technological interest due to their low melting temperatures (700–800 °C) [1], good optical transmission in the visible and infrared regions (up to about 6 μm) [2], high refractive indices (1.8–2.3), good resistance to hostile media when compared to hygroscopic fluorides, low phonon energy (~800 cm^{-1}) among oxide glasses, high dielectric constant (13 − 35) [3], and large third-order nonlinear susceptibility [4]. These properties make tellurite glasses suitable for applications involving third harmonic generation or optical Kerr effects [5–7]. Tellurite glasses are also strong candidates for super-high speed optical switches or shutters, and are promising materials for use in fiber optics [8] and solar cells [9,10,11] when they are doped and/or co-doped with rare earth or transition metal ions.

The transformation of pure tellurium oxide to glass is difficult, due to the presence of a pair of electrons in the equatorial region of the TeO_4 trigonal bipyramids (tbp) found in the tellurium oxide network [12,13]. This structural unit hinders creation of the structural arrangement necessary for glass formation. Therefore, it is very difficult to obtain pure tellurium oxide glass using the traditional melt-quenching process. In order to avoid this problem, alkali oxides have been added to TeO_2, which affects the optical properties of the glass, for example causing a blue shift in the absorption edge, and also improves the rare earth solubility [14,15]. When the ratio of the modifying oxide is increased, the dominant TeO_4 tbp structure is progressively converted into a TeO_3 trigonal pyramid (tp) structure [16].

It is well known that optical transitions between excited and ground states in ns^2-type ions are parity-allowed, with the atoms exhibiting ns^2 electron configuration in the excited state and ns^1np^1 electron configuration in the ground state [17]. Some examples of these atoms are Te^{4+}, Sn^{2+}, Sb^{3+}, Tl^{+}, Pb^{2+}, and Bi^{3+}. Among these, few reports can be found in the literature concerning Te^{4+} emissions. Donker et al. investigated the spectroscopic characteristics of Te^{4+}-doped alkali halides [18] and oxide crystals [19], while Masai et al. reported on the emission of Te^{4+}-doped zinc borate glass [20,21]. In these studies, it was found that Te^{4+} emission was strongly affected by the coordination field, mainly due to the electrons present in the outermost shell. This implies that the Te^{4+} emission intensity is strongly dependent on the temperature, so that at room temperature (RT) it is very low, with consequent low fluorescence quantum efficiency.

The fluorescence quantum efficiency (η), which is one of the most important optical parameters of luminescent ions, measures the conversion of absorbed photons into emitted photons. It can be determined using integration sphere or photothermal methods. In the latter case, the sample absorbs the energy from a laser and converts it into heat

* Corresponding author.
E-mail address: smlima@pesquisador.cnpq.br (S.M. Lima).

https://doi.org/10.1016/j.jlumin.2018.02.002
Received 13 November 2017; Received in revised form 31 January 2018; Accepted 1 February 2018
Available online 05 February 2018
0022-2313/

(non-radiative transitions). The fraction of the absorbed energy converted into heat, φ, is related to η, as will be discussed below. Among the photothermal methods, thermal lens spectroscopy (TLS) is an effective technique that has been used for determination of η in rare earth-doped glasses [22–24].

The aim of this study was to investigate whether Te^{4+} centers were present in lithium tellurite glass and to determine their fluorescence quantum efficiency at RT using thermal lens spectrometry (TLS). The main hypothesis was that during the processes of synthesis of lithium tellurite glasses, the TeO_2 acts as a conditional network former and can also be found in the matrix in ionic form (Te^{4+}).

2. Material and methods

Lithium tellurite glass with nominal composition $80TeO_2 - 20Li_2O$ (mol%) was prepared in an ambient atmosphere by the conventional melt-quenching method. The reagents TeO_2 (99.995% purity, Sigma-Aldrich) and Li_2CO_3 (99.997% purity, Sigma-Aldrich) were weighed out, mixed, and melted in a Pt-5%Au crucible at 850 °C for 1 h. The melt was poured into a stainless steel mold preheated to close to the glass transition temperature (T_g ~260 °C [25]) and was subsequently annealed for 5 h to relieve the mechanical tensions. The resulting glass was cut and polished. The sample density (ρ) was determined at room temperature by Archimedes' method, using distilled water as the immersion liquid, presenting a value of the (5.00 ± 0.01) g/cm^3.

The ground state absorption spectrum of the glass was obtained at RT using a UV–Vis spectrophotometer (Cary 50, Varian) operated in the wavelength range from 370 to 700 nm. The photoluminescence (PL) and PL excitation (PLE) spectra were obtained at RT, using a Xe lamp (150 W) as the excitation source, coupled to a monochromator (Newport Cornerstone 260™), mounted with a 300-line diffraction grating and blaze at 500 nm. The lamp emissions were selected with the Newport monochromator to excite the sample in the spectral range from 300 to 500 nm with step of the 5 nm. The luminescence of the sample was directed by an optical fiber to a second monochromator (iHR-320, Horiba Jobin Yvon) with aperture opening of 2 mm and operating with a diffraction grating of 600 lines and blaze at 600 nm. This second monochromator separated the wavelengths of the spectral emission band from 500 to 800 nm, with a 2 nm step, and directed the luminescent signal to the photomultiplier (R928, Hamamatsu). The obtained photoluminescence spectra are normalized by the Xe lamp to prepare an excitation-emission contour plot. Measurements of the lifetimes of Te^{4+} ions were obtained using excitation at wavelengths of 360 or 460 nm with an optical parametric oscillator (OPO) pumped by a 10 ns pulsed Nd:YAG laser (355 nm, 10 Hz).

The fluorescence quantum efficiency was determined by TLS, where the change in the probe beam intensity was proportional to the thermal lens-induced phase shift, given by [26]:

$$\theta = -\frac{P_{abs}}{K\lambda_p}\varphi\frac{ds}{dT}, \quad (1)$$

where $P_{abs} = P_e\alpha L_{eff}$ is the absorbed power, P_e is the excitation power, α is the optical absorption coefficient at λ_{exc}, $L_{eff} = [1\text{-}\exp(-\alpha L)]/\alpha$ is the effective sample thickness, L is the sample thickness, $K = \rho CD$ is the thermal conductivity, ρ is the volumetric density, C is the specific heat, D is the thermal diffusivity, $\varphi = 1\text{-}\eta(\lambda_{exc}/ < \lambda_{em} >)$ is the fraction of the absorbed energy converted into heat, $< \lambda_{em} >$ is the average emission wavelength, and ds/dT is the temperature coefficient of the optical path length at the probe beam wavelength, λ_p. The TLS setup consisted of two beams in a mode-mismatched configuration, with an excitation beam from an Ar^+ laser (Innova 308 C, Coherent) tuned at 360 nm and a probe beam from a HeNe laser at 632.8 nm. The transient curves obtained were fitted using the theoretical model proposed by Shen et al. [26]. Further details of the experimental arrangement can be found elsewhere [23].

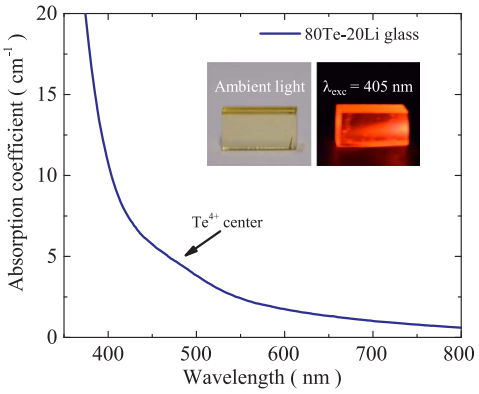

Fig. 1. Absorption coefficient spectrum of the $80TeO_2 - 20Li_2O$ glass at room temperature. The photographs in the inset are of the sample in ambient light and with excitation at 405 nm.

3. Results and discussion

Fig. 1 shows the UV–Vis–NNIR absorption coefficient spectrum of the 80Te-20Li glass, which was made in the form of a thin piece (L = 350 μm) polished to a high level of quality. A small feature in the absorption spectrum can be observed at around 480 nm, which overlapped with the initial part of the charge transfer band of the glass. The hypothesis was that this absorption was related to the Te^{4+} ions. The inset in Fig. 1 shows a photograph of the glass exposed to ambient light (yellow color) and excited at 405 nm using a diode laser. This unexpected observation, together with intense luminescence in the red region, has not been reported previously for lithium tellurite glass.

The dependence of the emission on the UV–Vis excitation was investigated by subjecting the glass to PL-PLE measurements. In Fig. 2(a), the excitation wavelength is plotted on the x-axis and the emission on the y-axis, and the intensity is shown using a log color scale. The contours show a broad range of emission in the visible and near-near infrared regions, between 500 and 800 nm, for excitation in the range from 300 to 500 nm. The maximum emission was at around 645 nm, for maximum excitation between 330 and 400 nm. There was a blue shift in the emission center position when the excitation was performed using higher energies (for wavelengths < 330 nm). Figs. 2(b) and 2(c) show the normalized PL spectra under excitation at 310, 360, and 460 nm, and the normalized PLE spectra for the emissions at 575 and 645 nm. For excitation at both 360 and 460 nm, there were broad emission bands (FWHM ~3400 cm^{-1}) with maxima centered at ~645 nm, while excitation at 310 nm resulted in a broad emission band (FWHM ~3900 cm^{-1}) centered at ~575 nm. This indicated that the luminescence of the glass could arise from two different states, with the emissions for excitation at 360 and 460 nm originating from the same band, while the emission for excitation at 310 nm originated from a second band. The PLE spectrum, shown in Fig. 2(c), presented a shape similar to those reported in the literature for Te^{4+}-doped materials [18,20,21].

To determine the fluorescence quantum efficiency of the Te^{4+} ion in the 80Te-20Li glass, thermal lens transient signals were obtained for excitation at 360 nm using different power levels. Fig. 3 shows a typical transient ($I(t)/I_o$) for excitation power of 11.3 mW. The experimental curve was fitted by the theoretical model proposed by Shen et al. [26], from which the parameters θ and t_c were determined. From the average value obtained for t_c (1.34 ± 0.01 ms), the thermal diffusivity ($D = \omega_{oe}^2/4t_c$, where in the setup used, ω_{oe} = 38 ± 1 μm) was calculated to be (2.7 ± 0.1) 10^{-3} cm^2/s. This was in agreement with the value reported in the literature for 80Te-20Li glass [27].

Plotting of the θ values as a function of the excitation power (P_e) confirmed the expected linear behavior (inset of Fig. 3), so a linear fit was performed to obtain the thermal lens amplitude signal normalized

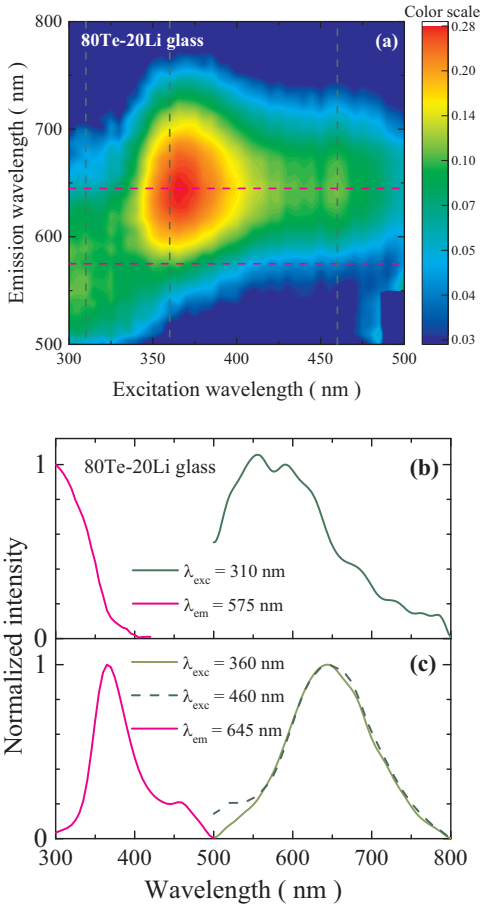

Fig. 2. (a) Excitation-emission contour plot for the $80TeO_2 - 20Li_2O$ glass at room temperature. (b) PL (right) spectrum with excitation at 310 nm and PLE (left) spectrum for emission observed at 575 nm. (c) PL (right) spectra with excitations at 360 and 460 nm and PLE (left) spectrum for emission observed at 645 nm.

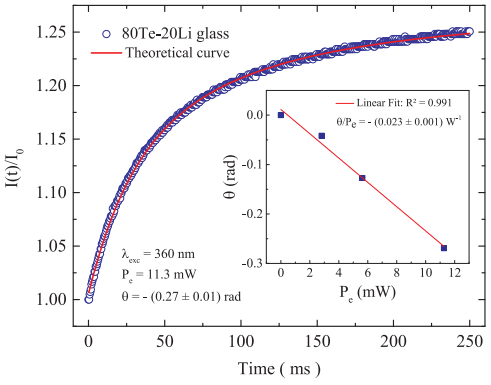

Fig. 3. Thermal lens transient signal for the $80TeO_2 - 20Li_2O$ glass with excitation at 360 nm. Inset: Thermal lens strength versus excitation power.

by the excitation power, $\theta/P_e = -0.023 \pm 0.001\,W^{-1}$. Use of the expression $\Theta = \theta/P_{abs}$ [24] resulted in $\Theta_{lum} = 23.3\,W^{-1}$ for the luminescent Te^{4+} centers in the 80Te-20Li glass. Since it is known that $\Theta_{nlum} = 36\,W^{-1}$ for the host glass without luminescence, as recently measured by the multi-wavelength method for Yb^{3+}-doped $80TeO_2 - 20Li_2O$ glass [24], the value for the fraction of the absorbed energy converted into heat could be obtained directly using $\Theta_{lum}/\Theta_{nlum} = (\theta/P_{abs})_{lum} \times \varphi/(\theta/P_{abs})_{nlum} = \varphi = 0.647 \pm 0.002$. Thus, considering the average emission wavelength $<\lambda_{em}> = 645$ nm, $\lambda_{exc} = 360$ nm, and the relation $\varphi = 1 - \eta(\lambda_{exc}/<\lambda_{em}>)$, a fluorescence quantum efficiency of $\eta = 0.63 \pm 0.06$ was obtained for Te^{4+}. This

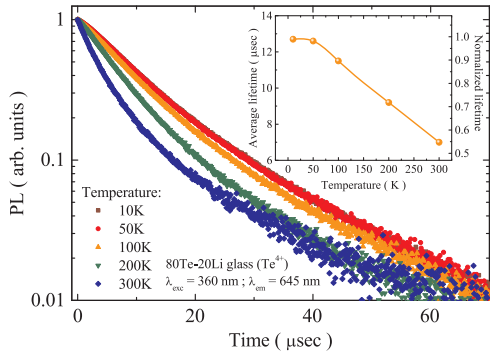

Fig. 4. Emission decay curves for the $80TeO_2$-$20Li_2O$ glass, as a function of temperature, with excitation at 360 nm. The inset shows the temperature dependence of the average lifetime (left axis) and the normalized lifetime (right axis).

value is very high, compared to the values reported previously for Te^{4+}-doped zinc borate glass (between 5% and 8%, with lifetime of ~3 μs) [21]. This difference was probably due to the limited local distribution of the Te^{4+} coordination state, with Te^{4+} in the 80Te-20Li glass structure expected to exhibit single symmetry. The η value obtained for the Te^{4+} center in lithium tellurite glass is comparable to the values measured for other ns^2 centers. Masai et al. found $\eta = 0.6$ (with lifetime of 5.5 μs) for Sn^{2+}-doped zinc borate glass [21]. The same authors noted that Te^{4+} PL is very difficult to observe at RT and that the fluorescence characteristics can vary with the local coordination field, depending not only on the chemical composition of the host glass, but also on the solidified cooling process [20,21].

The temperature dependence of the fluorescence signal was investigated in order to confirm the high η value for Te^{4+} in the 80Te-20Li glass. Fig. 4 shows the decay time curves for emission at 645 nm, with excitation at 360 nm, for sample temperatures ranging from 10 to 300 K. At low temperature, the curves were approximately single exponential, while non-exponential behavior occurred at higher temperature, indicating a decrease in the average lifetime of the sample. The inset of Fig. 4 shows the average lifetime for each temperature. Taking into account the Arrhenius behavior of the lifetime dependence with the temperature, the activation temperature is 405 K, which implies that the activation energy is 281.5 cm^{-1}. Between 10 and 300 K, the average lifetime decreased by approximately 45% (from 12.7 to 7 μs), indicating that at RT, η was ~55%, confirming the high value obtained by TLS for η in the tellurite glass. It is worth noting that at 300 K, the average lifetime was ~21% higher than the value reported for Sn^{2+}-doped zinc borate glass [21]. Although this comparison is not ideal, it shows that for an ns^2 center emission with long lifetime (longer than 5 μs), the fluorescence quantum efficiency is expected to be high. An additional explanation for the long lifetime obtained for Te^{4+} in lithium tellurite glass is that this glass matrix has a phonon energy of ~750 cm^{-1}, which is lower than the values for borate glasses (~1350 cm^{-1}) [28]. Furthermore, the Te^{4+} concentration in the glass was expected to be very low, so the fluorescence quenching effect was reduced.

As mentioned before, the shapes of the Te^{4+} PL spectra for excitation at 360 and 460 nm were similar (Fig. 2c), suggesting that the transition to the ground state originated in the same band for these excitation energies. To confirm this, decay time curves were performed at RT and the lifetime values obtained were 7.0 ± 0.3 and 6.5 ± 0.3 μs for excitations at 360 and 460 nm, respectively. This indicated that the red emission was derived from the same state, in this case the $^3T_{1u}$ level of the Te^{4+} center.

Based on the spectroscopic results, a partial energy level diagram for Te^{4+} was constructed (Fig. 5) in order to summarize the findings. For better understanding, the absorption and excitation spectra from Figs. 1 and 2 are also shown in Fig. 5. When an ultraviolet laser is used to excite the system (at around 260 nm, for example), an electron of the

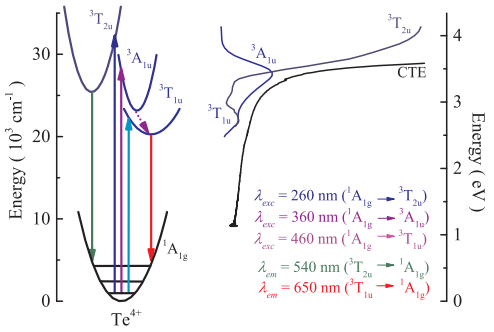

Fig. 5. Partial energy levels diagram of the Te^{4+} ion in lithium tellurite glass.

Te^{4+} ion is excited from the $^1A_{1g}$ ground state to the $^3T_{2u}$ excited state. From there, it decays via phonons to the band bottom and emits a broad emission band centered at ~575 nm (see Fig. 2). As there is an overlap between the charge transfer energies (CTEs) of the glass and the Te^{4+} center, the UV excitation also provides excitation of the tellurite glass, from where the electron can be transferred to the $^3T_{2u}$ excited state of the Te^{4+} center, which then relaxes radiatively to the ground state. The lifetime of the $^3T_{2u}$ excited state is very short (< 1 ns) so that it was not registered. For excitation at 360 nm ($^1A_{1g} \rightarrow {}^3A_{1u}$), the system relaxes via phonons from $^3A_{1u}$ to $^3T_{1u}$, from where it emits at around 645 nm ($^3T_{1u} \rightarrow {}^1A_{1g}$). No emission is expected for relaxation of $^3A_{1u}$ directly to the ground state, so the same emission shape and lifetime was observed for excitation at 460 nm.

These entire observed optical characteristic of tellurite glass indicates it for potential applications in photonics. As an example, as shown in Figs. 1 and 2 the glass exhibits a broad absorption band in the UV–Vis region of the electromagnetic spectrum, in a region where the solar spectrum has considerable irradiance. Together, the broad emission band in the red region can contribute to match the solar spectrum with the solar cell used actually. Materials with these characteristics have been looked to increase the efficiency in the conversion of the solar energy in electric one. Another possible application for tellurite glass is as low temperature sensor, mainly because it presents strong temperature dependence of the emission lifetime of Te^{4+}, as seen by the inset of Fig. 4.

4. Conclusions

In conclusion, the Te^{4+} center emission characteristic of lithium tellurite glass was observed. The $80TeO_2 - 20Li_2O$ glass presented a broad and intense emission spectrum at RT, which was related to the Te^{4+} centers, with lifetime and fluorescence quantum efficiency of 7.0 μs and 63%, respectively. This value of η is considered high, indicating that the glass has potential for photonic applications.

Acknowledgments

The authors are grateful for support provided by Fundação de Apoio ao Desenvolvimento do Ensino, Ciência e Tecnologia do Estado de Mato Grosso do Sul (FUNDECT – 23/200.735/2014), FAPESP, and the Brazilian National Research Council (CNPq).

References

[1] S. Sakida, S. Hayakawa, T. Yoko, Part 2.^{125}Te NMR study of M_2O-TeO_2 (M = Li, Na, K, Rb and Cs) glasses, J. Non-Cryst. Solids 243 (1999) 13–25.
[2] J. Heo, D. Lam, G.H. Sigel, E.A. Mendoza, D.A. Hensley, Spectroscopic analysis of the structure and properties of alkali tellurite glasses, J. Am. Ceram. Soc. 75 (1992) 277–281.
[3] J.S. Wang, E.M. Vogel, E. Snitzer, Tellurite glass: a new candidate for fiber devices, Opt. Mater. 3 (1994) 187–203.
[4] H. Niida, T. Uchino, J. Jin, Structure of alkali tellurite glasses from neutron diffraction and molecular orbital calculations, J. Chem. Phys. 114 (2001) 459–467.
[5] S.K. Lee, M. Tatsumisago, T. Minami, Fragility of liquids in the systems Li_2O- TeO_2, Phys. Chem. Glass. 35 (1994) 226–228.
[6] K. Putz, P.F. Green, Fragility in mixed alkali tellurites, J. Non-Cryst. Solids 337 (2004) 254–260.
[7] C.Y. Zahra, A.M. Zahra, Calorimetric studies of AgI-doped tellurite glasses, J. Non-Cryst. Solids 190 (1995) 251–257.
[8] M. Yamada, A. Mori, K. Kobayashi, H. Ono, T. Kanamori, K. Oikawa, Y. Nishida, Y. Ohishi, Gain-flattened tellurite-based EDFA with a flat amplification bandwidth of 76 nm, IEEE Photon, Technol. Lett. 10 (1998) 1244–1246.
[9] A. Pandey, R.E. Kroon, V. Kumar, H.C. Swart, Photon downshifting in strong NIR emitting Er^{3+}-Yb^{3+} embedded tungsten tellurite glass, J. Alloy. Compd. 657 (2016) 32–36.
[10] F.B. Costa, K. Yukimitu, L.A.O. Nunes, M.S. Figueiredo, J.R. Silva, L.H.C. Andrade, S.M. Lima, J.C.S. Moraes, High $Nd^{3+} \rightarrow Yb^{3+}$ energy transfer efficiency in tungsten-tellurite glass: a promising converter for solar cells, J. Am. Ceram. Soc. 100 (2017) 1956–1962.
[11] M.S. Figueiredo, F.A. Santos, K. Yukimitu, J.C.S. Moraes, L.A.O. Nunes, L.H.C. Andrade, S.M. Lima, On observation of the downconversion mechanism in Er^{3+}/Yb^{3+} co-doped tellurite glass using thermal and optical parameters, J. Lumin. 157 (2015) 365–370.
[12] H. Nasu, O. Matsushita, K. Kamiya, H. Kobayashi, K. Kubodera, Third harmonic generation from Li_2O-TiO_2-TeO_2 glasses, J. Non-Cryst. Solids 124 (1990) 275–277.
[13] J. Heo, D. Lam, G.H. Sigel Jr., E.A. Mendoza, D.A. Hensley, Spectroscopic analysis of the structure and properties of alkali tellurite glasses, J. Am. Ceram. Soc. 75 (1992) 277–281.
[14] M. Çelikbilek, A.E. Ersundu, S. Aydin, Preparation and characterization of TeO_2–WO_3–Li_2O glasses, J. Non-Cryst. Solids 378 (2013) 247–253.
[15] J.C. McLaughlin, S.L. Tagg, J.W. Zwanziger, The structure of alkali tellurite glasses, J. Phys. Chem. B 105 (2001) 67–75.
[16] E. Fargin, A. Berthereau, T. Cardinal, G. LeFlem, L. Ducasse, L. Canioni, P. Segonds, L. Sarger, A. Ducasse, Optical non-linearity in oxide glasses, J. Non-Cryst. Solids 203 (1996) 96–101.
[17] W.M. Yen, S. Shionoya, H. Yamamoto, Phosphor Handbook, 2nd ed., CRC Press, Boca Raton, 2007.
[18] H. Donker, W.M.A. Smit, G. Blasse, On the luminescence of Te^{4+} in A_2ZrCl_6 (A = Cs, Rb) and A_2SnCl_6 (A = Cs, Rb, K), J. Phys. Chem. Solids 50 (1989) 603–609.
[19] H. Donker, M.J. Den Exter, W.M.A. Smit, G. Blasse, Luminescence of the Te^{4+} Ion in ZrP_2O_7, J. Solid State Chem. 83 (1989) 361–365.
[20] H. Masai, Y. Yamada, S. Okumura, Y. Kanemitsu, T. Yoko, Photoluminescence of a Te^{4+} center in zinc borate glass, Opt. Lett. 38 (2013) 3780–3783.
[21] H. Masai, T. Yanagida, Photoluminescence of ns^2-type center-containing zinc borate glasses, J. Non-Cryst. Solids 431 (2016) 83–88.
[22] S.M. Lima, A.A. Andrade, R. Lebullenger, A.C. Hernandes, T. Catunda, M.L. Baesso, Multiwavelength thermal lens determination of fluorescence quantum efficiency of solids: application to Nd^{3+} doped fluoride glass, Appl. Phys. Lett. 78 (2001) 3220–3222.
[23] S.M. Lima, J.A. Sampaio, T. Catunda, A.C. Bento, L.C.M. Miranda, M.L. Baesso, Mode-mismatched thermal lens spectrometry for thermo-optical properties measurement in optical glasses: a review, J. Non-Cryst. Solids 273 (2000) 215–227.
[24] S.M. Lima, A.K.R. Souza, A.P. Langaro, J.R. Silva, F.B. Costa, J.C.S. Moraes, M.S. Figueiredo, F.A. Santos, M.L. Baesso, L.A.O. Nunes, L.H.C. Andrade, Fluorescence quantum yield of Yb^{3+} doped tellurite glasses determined by thermal lens spectroscopy, Opt. Mater. 63 (2017) 19–25.
[25] K. Yukimitu, R.C. Oliveira, E.B. Araújo, J.C.S. Moraes, L.H. Avanci, DSC studies on crystallization mechanisms of tellurite glasses, Thermochim. Acta 426 (2005) 157–161.
[26] J. Shen, J.R.D. Lowe, R.D. Snook, A model for cw laser induced mode-mismatched dual-beam thermal lens spectrometry, J. Chem. Phys. 165 (1992) 385–396.
[27] S.M. Lima, W.F. Falco, E.S. Bannwart, L.H.C. Andrade, R.C. de Oliveira, J.C.S. Moraes, K. Yukimitu, E.B. Araújo, E.A. Falcão, A. Steimacher, N.G.C. Astrash, A.C. Bento, A.N. Medina, M.L. Baesso, Thermo-optical characterization of tellurite glasses by thermal lens, thermal relaxation calorimetry and interferometric methods, J. Non-Cryst. Solids 352 (2006) 3603–3607.
[28] L. Ambrosi, M. Bettinelli, M. Ferrari, M. Casarin, A. Piazza, Optical spectroscopy of Eu^{3+} doped zinc borate glasses, J. Phys. Colloq. C4, Suppl. J. De. Phys. III 4 (1994) (C4-477 – C4-480).